

Supplemental Information

Figure S1. Related to Figure 1

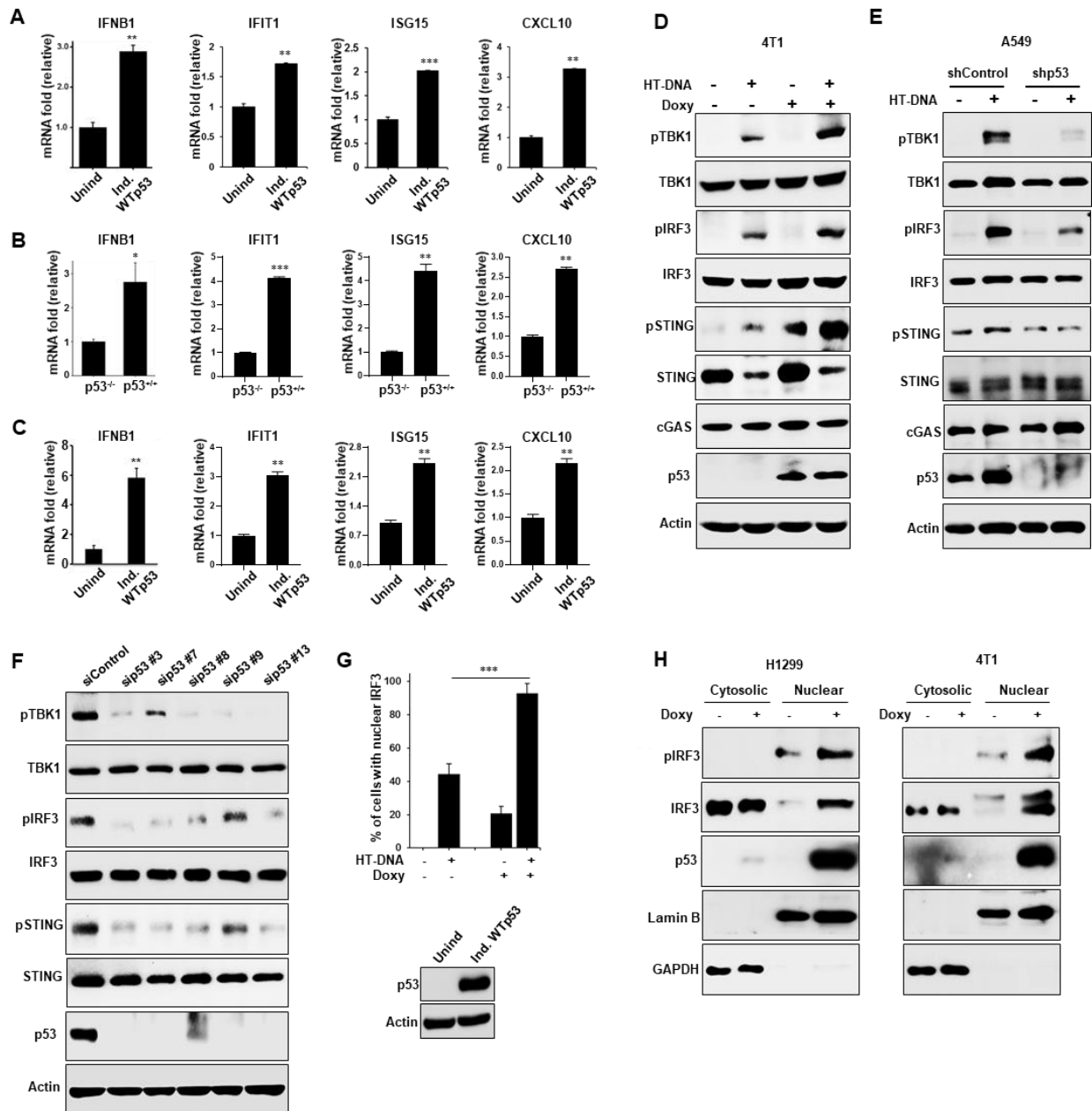


Figure S1. WTP53 activates cGAS/STING signaling, Related to Figure 1

(A-C) Graphs show mRNA expression of IFNB1, IFIT1, ISG15 and CXCL10 in (A) H1299 Induced WTP53 (B) p53^{+/+} and p53^{-/-} MEFs and (C) 4T1 Induced WTP53 cells. (D) 4T1 induced WTP53 cells were treated with 2 μ g/ml of HT-DNA for 3 h and subjected to western blot analysis. (E) shRNA mediated p53 knockdown (shControl or shp53) A549 cells were treated with 2 μ g/ml of HT-DNA for 3 h and cells were harvested for western blotting. (F) A549 cells were transfected with different p53 siRNAs (sip53) and subjected to Immunoblot analysis. (G) Stably GFP-IRF3

positive H1299 cells were engineered to inducibly express WTP53 upon doxycycline treatment. Cells were treated with Doxycycline for 24 h and then treated with HT-DNA (2 μ g/ml) for another 3 h. Representative graph shows quantitation of cells having nuclear IRF3 upon HT-DNA treatment. (Bottom) Western blot shows WTP53 induction upon doxycycline treatment. (H) Representative immunoblots of cytosolic and nuclear fractionated lysates of Doxycycline induced WTP53 in H1299 and 4T1 cells. GAPDH and Lamin B were used as loading controls for the cytoplasmic and nuclear fractions, respectively.

Quantification graphs: FoV=Field of View, (n=15) In all panels, error bars represent Mean +/- SD. p values are based on Student's t test. ***p < 0.001, **p < 0.01.

Figure S2. Related to Figure 2

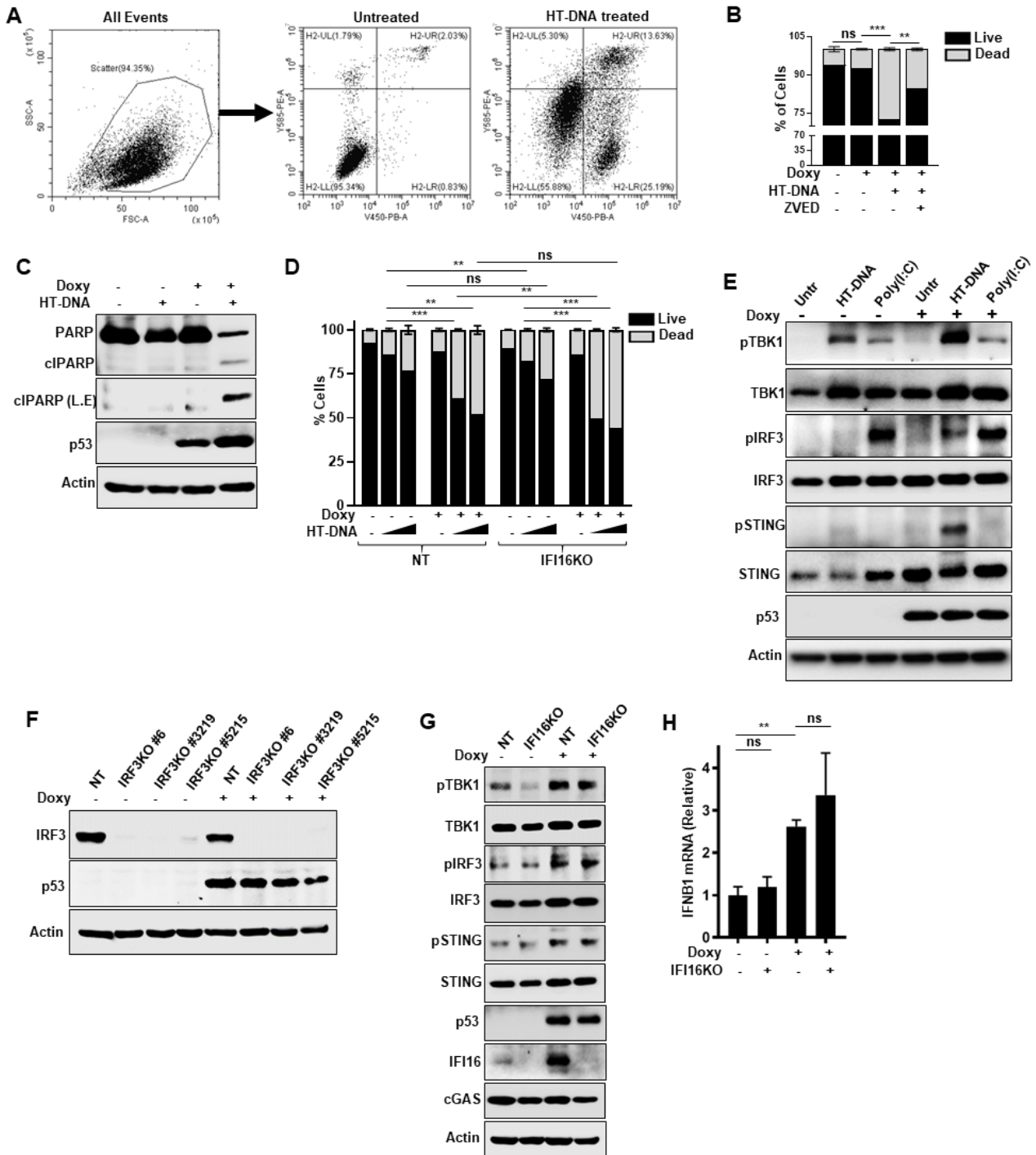


Figure S2. Wtp53 promotes cGAS/STING/IRF3 mediated apoptosis, Related to Figure 2

(A) Representative FACS scattered plots shows percent of cells going apoptosis after HT-DNA treatment. (B) H1299 cells were induced to express Wtp53 and then treated with HT-DNA and Caspase inhibitor (ZVED) and subjected to FACS analysis. (C) H1299 cells were induced to

express WTP53 and treated with HT-DNA for 24 hrs. Cells were harvested and subjected to western blot analysis. (D) non-target (NT) and IFI16KO H1299 cells induced WTP53 treated with 2 µg/ml or 4 µg/ml of HT-DNA for 24 h. Cells were harvested, stained with Annexin V-FITC and PI and subjected to flow cytometry analysis. (E) H1299 cells were induced to express WTP53 and treated with either HT-DNA or Poly(I:C) for 3 hrs. Cells were harvested and subjected to western blot analysis. (F) H1299 inducible WTP53 cells were stably knock out for IRF3. Cells were treated with doxycycline to induce WTP53 and subjected to Western blot. (G-H) H1299 inducible WTP53 cells were stably knock out for IFI16. Cells were treated with doxycycline to induce WTP53 and subjected to (G) Western blot or (H) cells were harvested and RT-PCR analysis was done for IFNB1.

Quantification graphs: In all panels, error bars represent Mean +/- SD. p values are based on Student's t test. ***p < 0.001, **p < 0.01, *p < 0.05.

Figure S3. Related to Figure 3

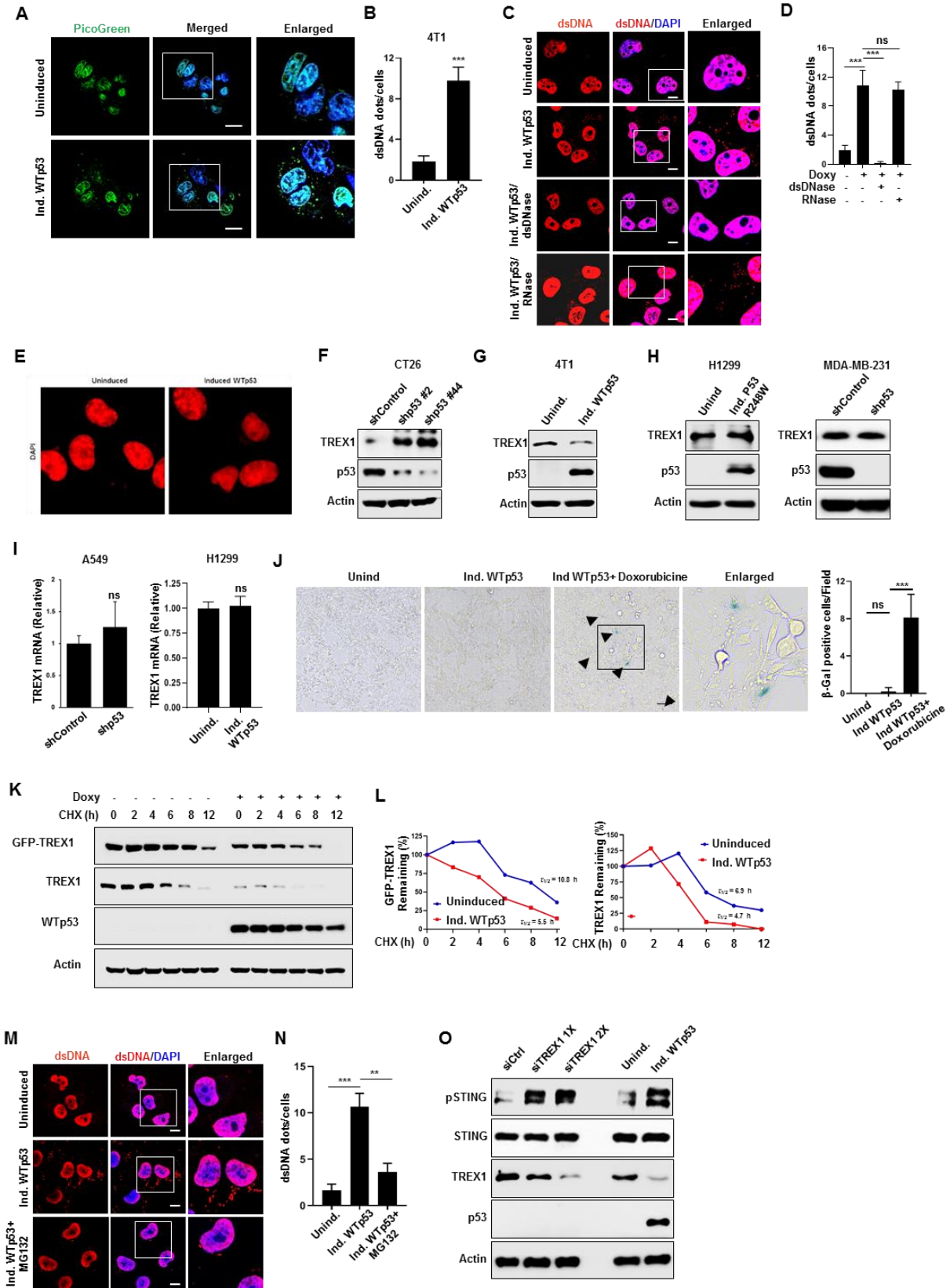


Figure S3. WTp53 promotes TREX1 degradation resulting in cytosolic DNA accumulation, Related to Figure 3

(A) Representative live confocal microscopy images of 4T1 induced WTp53 cells stained for cytosolic DNA using PicoGreen dye and the nucleus was stained with Hoechst 33342. Scale Bar 10 μ m. (B) Representative graph indicates quantitation of cytosolic DNA per cells. (C) Representative CLSM images showing dsDNA in H1299 cells induced WTp53 treated with dsDNase or RNase. (D) Representative graph shows quantitation of dsDNA per cells in the indicated cohorts. (E) Representative Fluorescence Microscopic images showing DAPI staining of H1299 induced WTp53 cells. (F) CT26 shControl or shp53 cells were subjected to western blot. (G) Representative Immunoblots of 4T1 cells induce WTp53. (H) Representative immunoblots of H1299 induced p53R248W and MDA-MB-231 shp53 cells. (I) Representative graphs shows TREX1 mRNA in A549 shControl or shp53 and H1299 induced WTp53 cells. (J) Representative bright field images showing β -Galactoside staining in the indicated cohorts. Representative graph indicating quantitation of β -Galactoside positive cells per field in the indicated cells. Scale Bar 25 μ m. (K) Representative immunoblots showing H1299 cells were induced to express WTp53 and treated with cycloheximide (20 μ M). Cells were harvested at the indicated different time point and subjected to western blot analysis. (L) Representative graphs indicate quantification of the relative levels of remaining GFP-TREX1 and endogenous TREX1 protein after the cycloheximide treatment described. (M) Representative CLSM images showing dsDNA in H1299 cells induced WTp53 treated with MG132. Scale Bar 10 μ m. (N) Representative graph indicates quantitation of cytosolic DNA per cells. (O) H1299 cells were transfected with different amount of TREX1 siRNA and H1299 cells were treated with Doxycycline to induce WTp53. Cells were harvested and subjected to western blot analysis.

Quantification graphs: In all panels, error bars represent Mean +/- SD. p values are based on Student's t test. ***p < 0.001, **p < 0.01, *p < 0.05, ns=non-significant. Scale bar 10 μ m.

Figure S4. Related to Figure 4

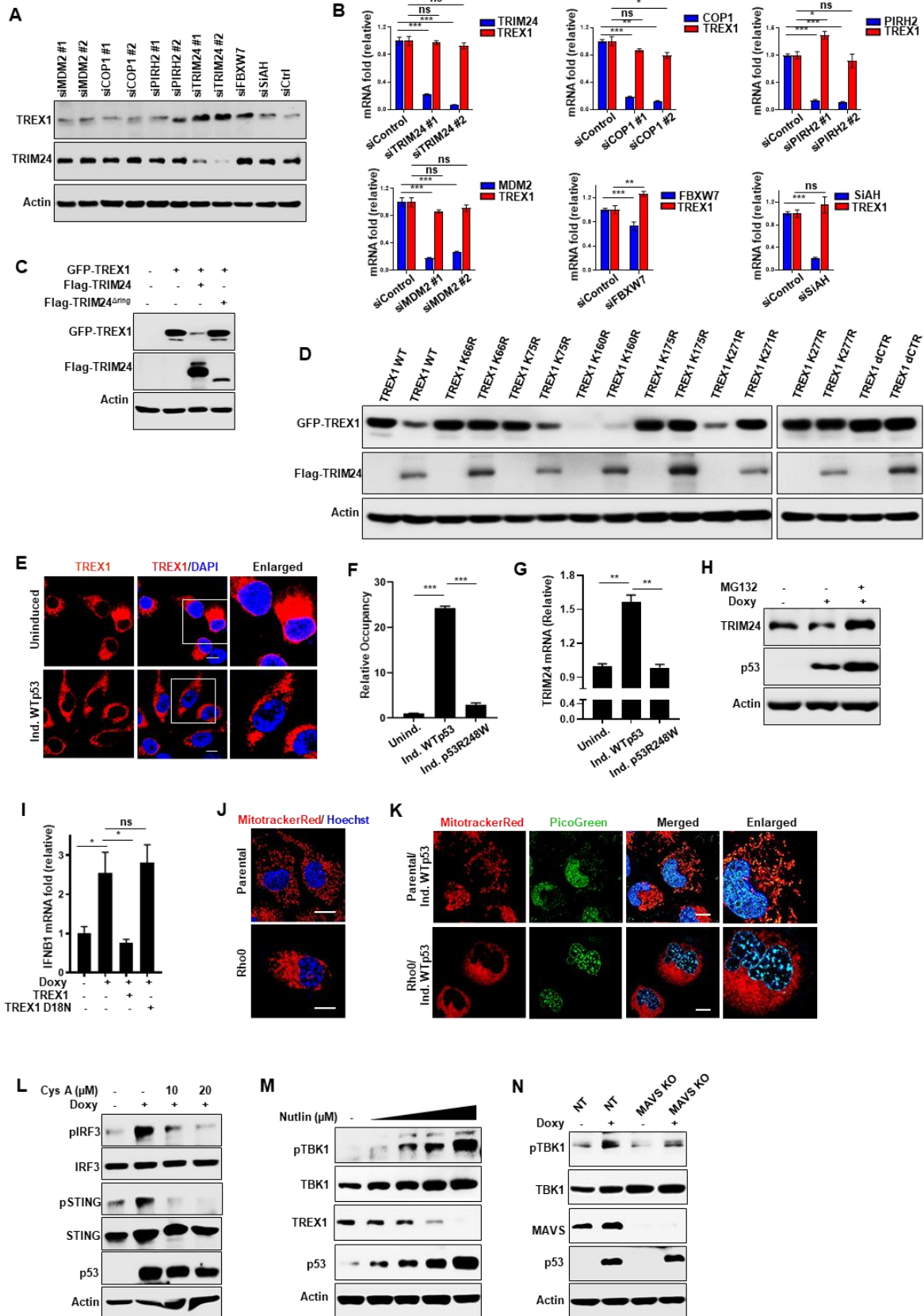


Figure S4. TRIM24 is an ubiquitin ligase for TREX1, Related to Figure 4

H1299 cells were transfected with siRNAs of MDM2, COP1, PIRH2, TRIM24, FBXW7 and SiAH. Cells were harvested and subjected to (A) western blot analysis or (B) RT-PCR for the indicated genes. (C) H1299 cells were co-transfected with GFP-TREX1 and Flag-TRIM24 or Flag-TRIM24^{Δring} and subjected to western blot. (D) GFP-TREX1 or different GFP-TREX1 lysine mutants were transfected in H1299 cells with or without Flag-TRIM24. Cells were harvested and subjected to western blot analysis. (E) Representative confocal immunofluorescence images are showing TREX1 localization in H1299 induced WTP53 cells. Scale Bar 10μM. (F) Representative chromatin immunoprecipitation (ChIP) data showing relative occupancy of WTP53 or p53R248W in the TRIM24 promoter region. (G) Representative graph indicate TRIM12 mRNA in H1299 cells were induced to express either WTP53 or p53R248W. (H) H1299 cells were induced to express WTP53 and treated with MG132 and subjected to western blot analysis. (I) H1299 induced WTP53 stably overexpress GFP-TREX1 or GFP-TREX1 D18N cells were lysed and subjected to RT-PCR analysis. (J) Representative Confocal microscopic images showing MitotrackerRed staining in H1299 parental and Rhoo cells. (K) H1299 parental and Rhoo cells were induced to express WTP53 and stained for MitotrackerRed to visualize mitochondria and Picogreen to stain cytosolic DNA. Scale Bar 10μM. (L) H1299 inducible WTP53 cells were treated with doxycycline to express WTP53 and treated with Cyclosporine A (CysA) and subjected to western blot analysis. (M) A549 cells were treated with increasing amount of Nutlin for 24 hrs and are subjected to western blot. (N) H1299 inducible WTP53 cells were engineered to CRISPR knockout MAVS and subjected to western blot.

Quantification graphs: In all panels, error bars represent Mean +/- SD. p values are based on Student's t test. ***p < 0.001, **p < 0.01, *p < 0.05.

Figure S5. Related to Figure 5

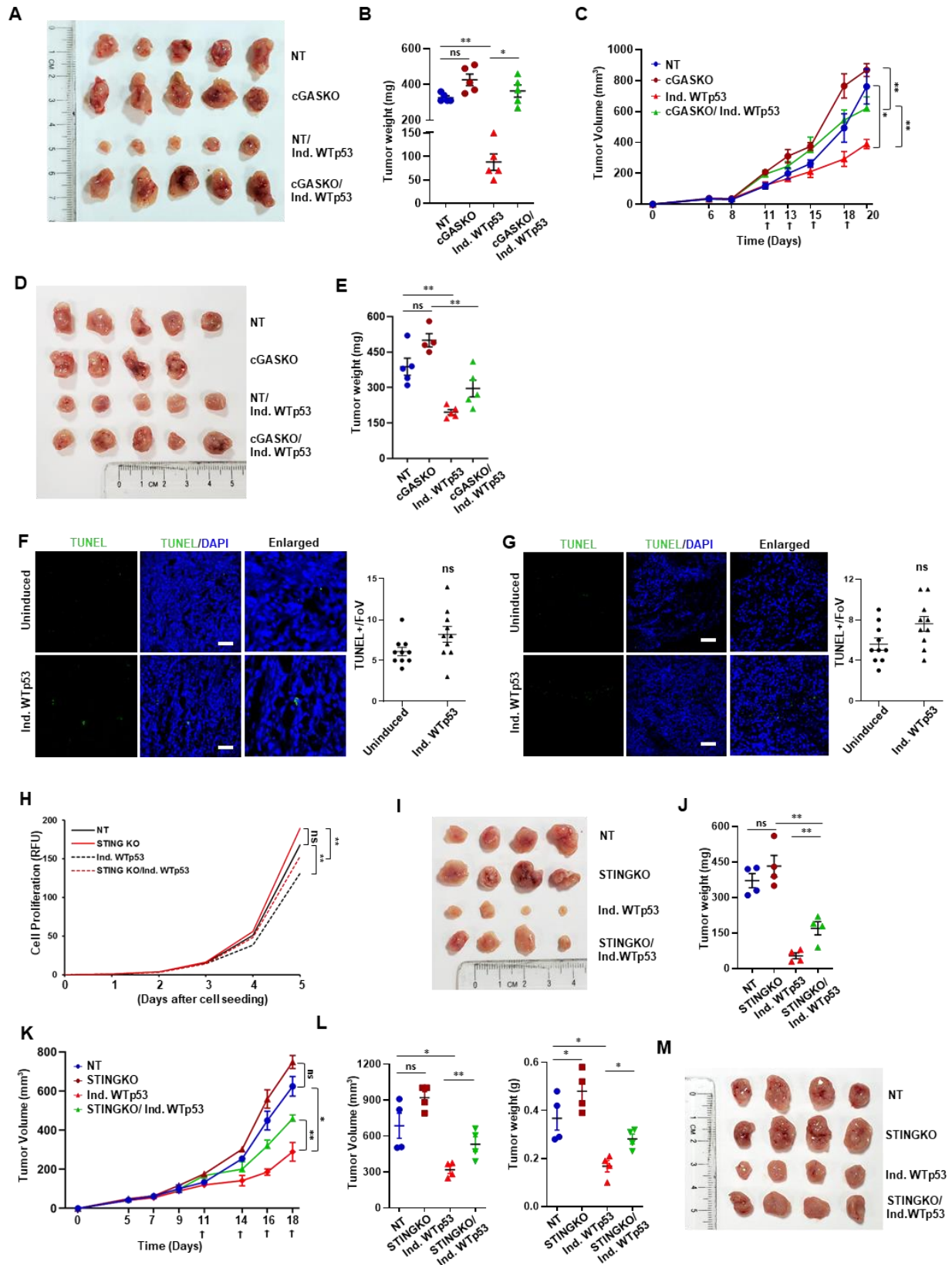


Figure S5. WTP53 promotes cGAS/STING dependent antitumor immune response, Related to Figure 5

(A) Representative images showing tumor volume difference of 4T1 induced WTP53 non-target (NT) or cGAS knockout cells in BALB/c mice. (B) Graphical quantification of tumor weight on day 23 in the indicated 4T1 tumor cohorts in BALB/c mice (n= 4). (C) 5×10^4 4T1 induced WTP53 non-target (NT) or cGAS knockout cells were injected into the of mammary gland of immunodeficient NOD/SCID mice (n=5). Mice were orally given doxycycline to induce WTP53 (indicated by arrow). All mice were sacked on day 21 and graphical quantification represents the tumor growth rate. (D) Representative images showing tumor volume difference of 4T1 induced WTP53 non-target (NT) or cGAS knockout cells in NOD/SCID mice. (E) Graphical quantification of tumor weight on day 21 in the indicated 4T1 tumor cohorts in NOD/SCID mice (n= 5). (F) Representative immunostaining for tumor cell death (TUNEL) in 4T1 uninduced and Ind. WTP53 tumor sections in Balb/C mice. scale bar 25 μ m. (Right) Representative graph showed quantification of TUNEL positive cells. (n=10) (G) Representative immunostaining for tumor cell death (TUNEL) in 4T1 uninduced and Ind. WTP53 tumor sections in NOD/SCID mice. scale bar 25 μ m. (Right) Representative graph showed quantification of TUNEL positive cells. (n=10) (H) Representative graphical quantification of *in vitro* cellular proliferation rate between indicated 4T1 cells. (I) Representative images showing tumor volume difference of 4T1 induced WTP53 non-target (NT) or STING knockout cells in immunocompetent BALB/c mice (n=5). (J) Graphical quantification of tumor weight on day 23 in the indicated 4T1 tumor cohorts in BALB/c mice (n= 4). (K) 5×10^4 4T1 induced WTP53 non-target (NT) or STING knockout cells were injected into the of mammary gland of immunodeficient NOD/SCID mice (n=4). Mice were orally given doxycycline to induce WTP53 (indicated by arrow). All mice were sacked on day 21 and graphical quantification represents the tumor growth rate. (L) Graphical quantification of tumor volume and weight on day 19 in the indicated 4T1 tumor cohorts in NOD/SCID mice (n= 4). (M) Representative images showing tumor volume difference of 4T1 induced WTP53 non-target (NT) or STING knockout cells in immunodeficient NOD/SCID mice (n=4).

Quantification graphs: In all panels, error bars represent Mean +/- SEM. p values are based on Student's t test. ***p < 0.001, **p < 0.01, *p < 0.05.

Figure S6. Related to Figure 6

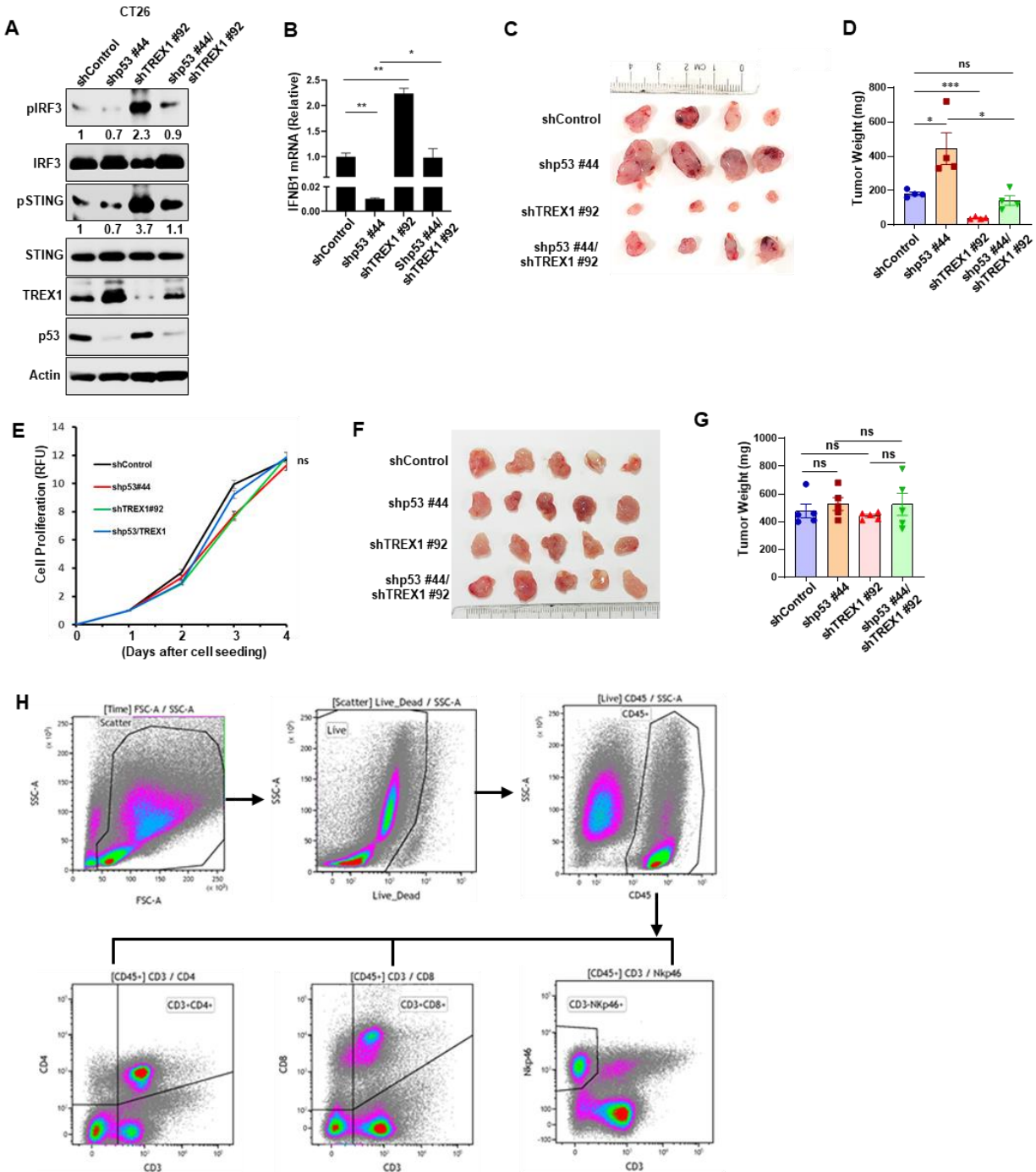


Figure S6. TREX1 deficiency induces WTp53 dependent antitumor immune response, Related to Figure 6

(A) CT26 cells were infected to knockdown either p53 or TREX1 alone or together and subjected to western blot analysis. (B) CT26 shp53, shTREX1 or shp53/shTREX1 cells were subjected to RT-PCR analysis. (C) Representative image showing tumor volume difference of CT26 shp53, shTREX1 or shp53/shTREX1 cells in BALB/c mice. (D) Graphical quantification of difference in

tumor weight on day 20 in shp53, shTREX1 or shp53/shTREX1 cohorts (n= 4). (E) Representative graphical quantification of *in vitro* cellular proliferation rate between indicated CT26 shp53, shTREX1 or shp53/shTREX1 cells. (F) Representative image showing tumor volume difference of indicated CT26 cohorts in NOD/SCID mice. (G) Graphical quantification of tumor weight on day 14 in CT26 shp53, shTREX1 or shp53/shTREX1 cohorts in NOD/SCID mice (n= 5). (H) Gating strategy to identify lymphoid immune populations. Scatter plots depicting population of live population of cells isolated from tumors based on FSC and SSC. Following the scatter gate, cells were further gated to identify live CD45+ cells. CD45+ cells were plotted on a scatter dot plot to identify CD3+CD4+ population (T-helper), CD3+CD8+ cells (T-cytotoxic) and CD3-Nkp46+ cells (NK).

Figure S7. Related to Figure 6

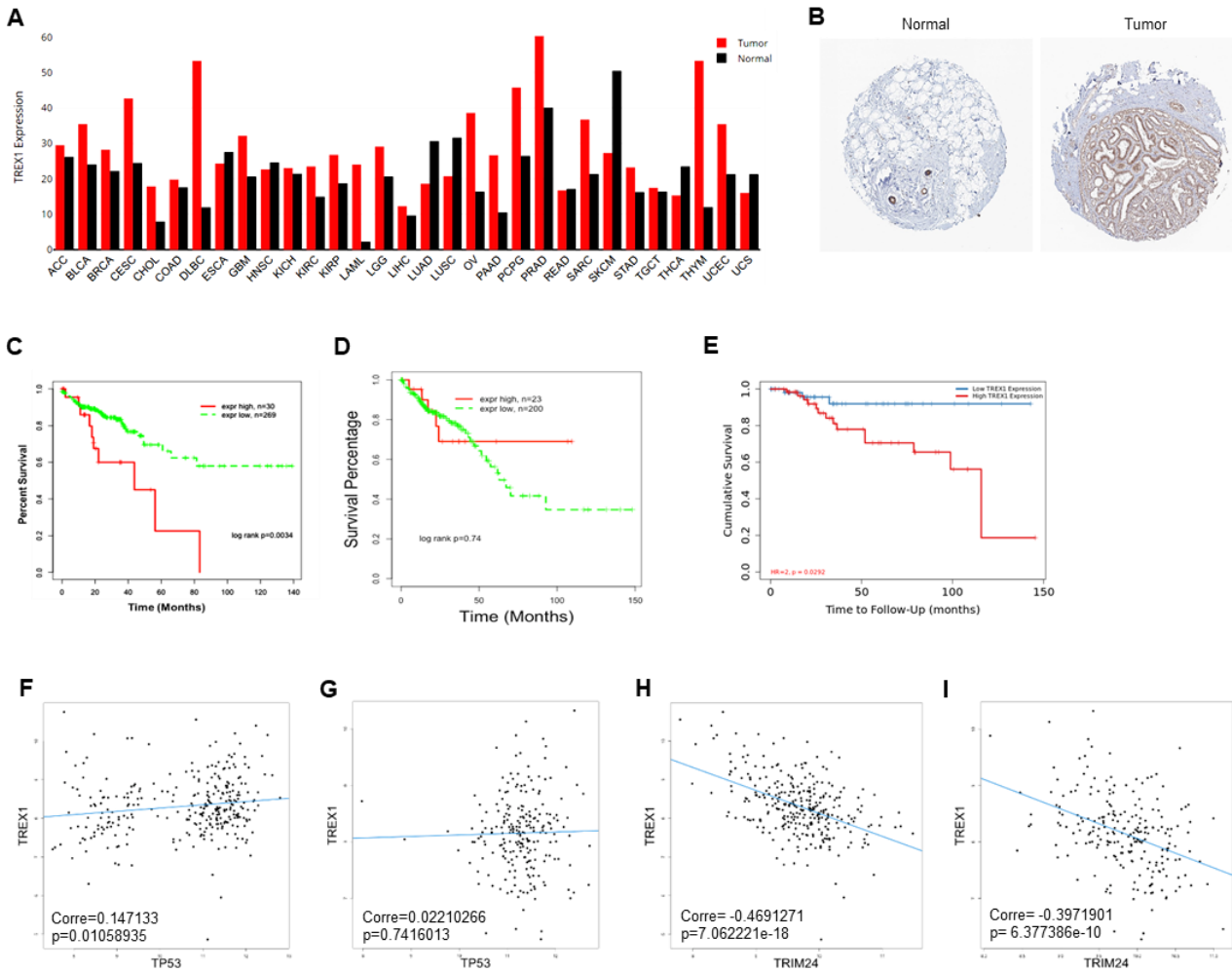


Figure S7. TREX1 overexpression correlates with tumor aggressiveness, Related to Figure 6:

(A) Expression of TREX1 in different tumor types was determined using the GEPIA (<http://gepia.cancer-pku.cn/index.html>) databases. (B) Immunohistochemical staining of TREX1 protein in Breast cancer tissues and corresponding normal tissues was obtained from the Human Protein Atlas (HPA) database. (C) Kaplan–Meier survival curves from TCGA dataset comparing the high and low expression of TREX1 in WTp53 Colorectal cancer (D) Kaplan–Meier survival curves from TCGA dataset comparing the high and low expression of TREX1 in missense mutant p53 Colorectal cancer (E) Kaplan–Meier survival curves from TCGA dataset comparing the high and low expression of TREX1 in breast carcinomas (BRCA) as determined using the TIMER 2.0 database. (F–I) Correlation analysis of the TCGA colorectal carcinoma database showed the correlation between (F) TREX1 and p53 mRNA levels in WTp53 tumor. (G) TREX1 and p53 mRNA levels in mutant p53 tumor cohorts. (H) TREX1 and TRIM24 mRNA levels in WTp53 tumor. (I) TREX1 and TRIM24 mRNA levels in mutant p53 tumors.

Table S1: List of primers, Related to STAR methods

Gene name	Forward Primer	Reverse Primer	Comments
P53	ATATACGCGTATGGAGGAGCCG CAGT	ATATGGATCCTCAGTCTGAGTC AGGCCCTTCT	Inducible human WTp53
P53 #2	GTACATGTGTAATAGCTCC		shRNA targeting Mouse p53
P53 #44	CCACTACAAGTACATGTGTAA		shRNA targeting Mouse p53
TREX1 #92	CCTAGATGGTACCTTCTGTGT		shRNA targeting Mouse TREX1
cGAS	pLCRISPR-CMV-cGAS3, Addgene No: 102610		sgRNA targeting Human cGAS
STING	pLentiCRISPRv2- STING_gRNA3, Addgene No: 127640		sgRNA targeting Human STING
IRF3 #6	CACCGGTAGGCCTTGTACTGGT CGG		sgRNA targeting Human IRF3
IRF3 #3219	CACCGGACACCTCTCCGGACAC CAA		sgRNA targeting Human IRF3
IRF3 #5215	CACCGGCTGGTGTCCGAGCTGG ACC		sgRNA targeting Human IRF3
IFI16	CACCGTATACCAACGCTTGAAG ACC		sgRNA targeting Human IFI16
cGAS	GCGAGGGTCCAGGAAGGAAC PMID: 33372007		sgRNA targeting Mouse cGAS
STING	CTACATAACAACATGCTCAG PMID: 33372007		sgRNA targeting Mouse STING
MAVS	TGTCTTCCAGGATCGACTGC		sgRNA targeting Human MAVS
IFNB1 (h)	GTCAGAGTGGAAATCCTAAG	TATGCAGTACATTAGCCATC	qPCR primers
IFIT1 (h)	TACAGCAACCATGAGTACAA	TCACATAGGCTAGTAGGTTG	qPCR primers
ISG15 (h)	GAATCATCTTTGCCAGTA	ATCTTCTGGGTGATCTGC	qPCR primers
CXCL10 (h)	TACCTGCATCAGCATTAGTA	TGTAGCAATGATCTCAACAC	qPCR primers
IFNB1 (m)	AAGATCAACCTCACCTACAG	AAAGGCAGTGTA ACTCTTCT	qPCR primers
IFIT1 (m)	AGCTATGTCATTGCTATG	GCCCTTTTGTATAATGTAAG	qPCR primers
ISG15 (m)	ACAGTGATGCTAGTGGTACA	AAGACCTCATAGATGTTGCT	qPCR primers
CXCL10 (m)	AAGTTTACCTGAGCTCTTTT	AGTATCTTGATAACCCCTTG	qPCR primers

TREX1 (h)	TCTGTGTGGATAGCATCA	AGGCTATAGCTCTTCCTTG	qPCR primers
TRIM24 (h)	GACACAATCTCCAAAATGAAT	TCTTCAGGTTTCAGTCTTCAGT	qPCR primers
PIRH2 (h)	AAAACGTGGAATTTGTAGG	GGGACACATTTTCAATACA	qPCR primers
FBXW7 (h)	CCTTTGCATCTTCTGATAGT	ACACGATTCATCTGTTCTTC	qPCR primers